

This article is licensed under a Creative Commons Attribution-NonCommercial NoDerivatives 4.0 International License.

## Experimental and In Silico Analysis of Cordycepin and its Derivatives as Endometrial Cancer Treatment

Pedro Fong,<sup>\*1</sup> Cheng N. Ao,<sup>\*†1</sup> Kai I. Tou,<sup>\*</sup> Ka M. Huang,<sup>\*</sup> Chi C. Cheong,<sup>\*</sup> and Li R. Meng<sup>\*</sup>

<sup>\*</sup>School of Health Sciences, Macao Polytechnic Institute, Macao, P.R. China

<sup>†</sup>State Key Laboratory of Quality Research in Chinese Medicine, Macau University of Science and Technology, Macao, P.R. China

The aim of this study was to investigate the inhibition effects of cordycepin and its derivatives on endometrial cancer cell growth. Cytotoxicity MTT assays, clonogenic assays, and flow cytometry were used to observe the effects on apoptosis and regulation of the cell cycle of Ishikawa cells under various concentrations of cordycepin, cisplatin, and combinations of the two. Validated in silico docking simulations were performed on 31 cordycepin derivatives against adenosine deaminase (ADA) to predict their binding affinities and hence their potential tendency to be metabolized by ADA. Cordycepin has a significant dose-dependent inhibitory effect on cell proliferation. The combination of cordycepin and cisplatin produced greater inhibition effects than did cordycepin alone. Apoptosis investigations confirmed the ability of cordycepin to induce the apoptosis of Ishikawa cells. The in silico results indicate that compound MRS5698 is least metabolized by ADA and has acceptable drug likeness and safety profiles. This is the first study to confirm the cytotoxic effects of cordycepin on endometrial cancer cells. This study also identified cordycepin derivatives with promising pharmacological and pharmacokinetic properties for further investigation in the development of new treatments for endometrial cancer.

**Key words: Adenosine deaminase; Cordycepin; Docking; Endometrial cancer; Herbal medicines**

### INTRODUCTION

Endometrial cancer is one of the most common female malignancies worldwide. The number of new diagnoses is increasing every year, and the age at diagnosis is falling<sup>1</sup>. In China, endometrial cancer is the second most common cancer of the female reproductive system after cervical cancer<sup>2</sup>. In the US and Europe, endometrial cancer has one of the highest morbidity rates among the female reproductive system cancers. According to the US National Cancer Institute, about 710,228 women had endometrial cancer in 2014<sup>3</sup>. It is estimated that the number of new cases will increase in the future.

Surgical treatment is one of the most common therapeutic strategies for endometrial cancer. It may be combined with radiotherapy to enhance the efficacy of treatment. As an adjuvant therapy, chemotherapy can enhance the survival rate of patients with endometrial cancer. However, most chemotherapeutics are not specific to cancer cells and are harmful to healthy cells, generally with dose-dependent cytotoxic effects. Hence,

chemotherapy has many side effects that are known to affect patients' quality of life. Another concern of chemotherapy is drug resistance, which means a higher dosage is required for the same therapeutic response, and this certainly increases the level of adverse reactions. Novel treatments are thus required to replace chemotherapy or to reduce its required dose.

In recent years, traditional Chinese medicine (TCM) has become popular in cancer therapy. According to a review of previous studies, TCM can induce cellular apoptosis, suppress tumor metastasis, reduce opportunities for multi-drug resistance, and produce immunomodulatory effects<sup>4</sup>. Although the pharmacological mechanisms of many TCM treatments are unclear, many therapeutic compounds have been developed by screening the active compounds in TCM herbs, some of which have shown antitumor effects<sup>5,6</sup>. For instance, cordycepin is an active component of *Cordyceps sinensis* that exhibits many clinical health effects including anti-inflammatory, immunomodulatory, antioxidant, and antimicrobial activities<sup>7</sup>. One study demonstrated the

<sup>1</sup>These authors provided equal contribution to this work.

Address correspondence to Li R. Meng, School of Health Sciences, Macao Polytechnic Institute, Meng Tak Building, Room 730, Rua de Luís Gonzaga Gomes, Macao, P.R. China. Tel: +853-85993449; Fax: +853-28753159; E-mail: [lrmeng@ipm.edu.mo](mailto:lrmeng@ipm.edu.mo)

anticancer effects of cordycepin in both in vivo and in vitro experiments and that cordycepin can induce cellular apoptosis and regulate the cell cycle in cervical cancer<sup>8</sup>. No evidence has yet confirmed the cellular apoptosis effects of cordycepin on endometrial cancer cells. The aim of this study was therefore to fill this research gap.

Several in vitro and animal studies have shown that *C. sinensis* exerts direct cytotoxicity against various types of cancer cells by inducing the activities of A<sub>3</sub> adenosine receptors (A<sub>3</sub>ARs)<sup>9</sup>. A<sub>3</sub>AR is a subtype of adenosine receptor that has been intensively studied for its role in cancer treatment. A<sub>3</sub>AR is a G<sub>i</sub> protein-associated molecule found in many human cells<sup>10</sup>. Its expression is significantly higher in inflamed cells and various cancer cells<sup>11,12</sup>. This overexpression of A<sub>3</sub>AR suggests the potential for the development of a biological marker and therapeutic agents for cancer and inflammatory diseases<sup>13</sup>. Studies have shown that stimulation of A<sub>3</sub>AR can disturb different cancer-related pathways, including WNT, PKA, MMPs, MAPK, and VEGF. Evidence shows that each of these pathways enhances tumor cell proliferation and that their disturbance may attenuate cancer cell growth. A<sub>3</sub>AR signaling is also linked to tumor metastasis. For instance, A<sub>3</sub>AR can inhibit the activities of telomerase and cell cycle arrest and produce cytostatic effects in lymphoma cells<sup>14</sup>. This mechanism is thought to explain muscle tissues' resistance to tumor metastasis<sup>15</sup>.

More than 50 adenosine receptor agonists have been developed<sup>16</sup>. They have various binding affinities and different levels of stimulation of different types of adenosine receptor, including A<sub>1</sub>AR, A<sub>2</sub>AR, A<sub>2</sub>BR, and A<sub>3</sub>AR. An agonist with high specificity to A<sub>3</sub>AR would mean less binding to other receptors and theoretically fewer side effects. Animal studies and phase II clinical trials have been conducted to validate the safety and efficacy of A<sub>3</sub>AR in inflammatory, ophthalmic, and liver diseases; melanoma; and prostate, colon, and hepatocellular carcinomas<sup>17</sup>. The results are promising. This further increases the possibility of finding an A<sub>3</sub>AR agonist as a new treatment for endometrial cancer, which was the aim of this study.

Cordycepin is thought to be the active ingredient responsible for producing the anticancer effects of *C. sinensis*. An in vitro study by Tao et al. demonstrated the ability of cordycepin to stimulate A<sub>3</sub>AR and hence produce direct cytotoxicity against lung carcinoma cells<sup>18</sup>. However, animal and clinical studies showed that cordycepin is rapidly and substantially metabolized by adenosine deaminase (ADA)<sup>19</sup>, leading to its unfavorable pharmacokinetic property of a short half-life. In purine metabolism, ADA deaminates adenosine to the inactive metabolite inosine<sup>20</sup>. One way to overcome this problem of rapid metabolism is to coadminister cordycepin with ADA inhibitors, such as cladribine and deoxycytosine, although this may

cause undesirable side effects<sup>21</sup>. Another way to increase the half-life of cordycepin is to modify its chemical structure to maintain the high specificity to A<sub>3</sub>AR along with low binding affinity to ADA.

The aim of this study was to identify cordycepin derivatives with promising pharmacological and pharmacokinetic properties for further investigation in the development of new treatments for endometrial cancer. We first confirmed the antitumor effects of cordycepin and that of its combination with cisplatin through MTT assays on endometrial cancer cells. We then used flow cytometry to observe the effects on apoptosis and regulation of the cell cycle of Ishikawa cells under various concentrations of cordycepin, cisplatin, and combinations of the two. After confirmation of the antitumor effects, we used computational docking simulations to calculate the binding affinities of a set of cordycepin derivatives against ADA, aiming to identify a compound with high potency on A<sub>3</sub>AR and resistance to ADA metabolism. The drug-like properties of these compounds were also predicted.

## MATERIALS AND METHODS

### Cell Culture

An Ishikawa cell line (ATCC, Manassas, VA, USA) was cultured in RPMI-1640 (11875; Gibco, Waltham, MA, USA) supplemented with 10% fetal bovine serum (FBS; 16000044; Gibco). The cells were cultured at 37°C in a humidified 5% CO<sub>2</sub> atmosphere.

### Cytotoxicity Assay

An MTT assay of 4 × 10<sup>3</sup> Ishikawa cells seeded in 96-well plates was performed to determine cell viability. The cells were then exposed to different concentrations of cordycepin (C3394; Sigma-Aldrich, Burlington, MA, USA), cisplatin (P4394; Sigma-Aldrich), and their combinations for 24 h (Table 1) and then washed carefully with PBS. Then 100 µl of culture medium with no FBS but MTT (1 mg/ml) was added, and the cells were held for 4 h at 37°C in a humidified 5% CO<sub>2</sub> atmosphere. The medium was removed, and formazan crystals were dissolved by adding 150 µl of DMSO (D4540; Sigma-Aldrich) and shaking for 15 min. Optical density (OD) was measured at 550 nm with a microplate reader (SPECTROstar Nano; Ortenberg, Allmendgrün, Germany), and the percentage of inhibition was calculated as follows: percentage viability = 100% × mean of test OD / mean of control OD and percentage inhibition = 100 – percentage viability.

### Clonogenic Survival Assay

Clonogenic assays were performed to determine the effectiveness of cordycepin and cisplatin on inhibiting the growth of Ishikawa cells. Combining the results

**Table 1.** Inhibition on Ishikawa Cells of Cordycepin, Cisplatin, and Their Combinations

Compounds (Concentration)	Inhibition Rate	<i>p</i> Values
Cordycepin (12.5 µg/ml)	4.7% ± 1.8%	0.02
Cordycepin (25 µg/ml)	9.7% ± 1.8%	<0.01
Cordycepin (50 µg/ml)	32.9% ± 1.2%	<0.01
Cordycepin (100 µg/ml)	57.1% ± 3.4%	<0.01
Cisplatin (0.5 µg/ml)	5.9% ± 2.4%	0.04
Cisplatin (1 µg/ml)	19.6% ± 2.4%	<0.01
Cisplatin (2 µg/ml)	29.6% ± 1.8%	<0.01
Cisplatin (4 µg/ml)	51.6% ± 1.4%	<0.01
Cordycepin (12.5 µg/ml) plus cisplatin (0.5 µg/ml)	21.3% ± 2.1%	0.04
Cordycepin (12.5 µg/ml) plus cisplatin (1 µg/ml)	26.6% ± 3.0%	0.02
Cordycepin (12.5 µg/ml) plus cisplatin (2 µg/ml)	34.8% ± 0.8%	0.02
Cordycepin (12.5 µg/ml) plus cisplatin (4 µg/ml)	76.8% ± 0.4%	<0.01
Cordycepin (25 µg/ml) plus cisplatin (0.5 µg/ml)	24.3% ± 2.6%	<0.01
Cordycepin (25 µg/ml) plus cisplatin (1 µg/ml)	33.7% ± 2.1%	<0.01
Cordycepin (25 µg/ml) plus cisplatin (2 µg/ml)	40.6% ± 1.5%	<0.01
Cordycepin (25 µg/ml) plus cisplatin (4 µg/ml)	80.1% ± 0.3%	<0.01

from the MTT assays with clonogenic assays can further enhance the reliability of our findings, as clonogenic assay determines the ability of cells to undergo division, while MTT assay determines cell viability.

A total of 200 Ishikawa cells were seeded in a 48-well plate for 24 h at 37°C in a humidified 5% CO<sub>2</sub> atmosphere. The cells were treated with cordycepin, cisplatin, and their combinations for 24 h, and then the cultural medium was replaced by the complete medium and incubated for 7 days. The cell colonies were stained with Wright–Giemsa stain (WG16; Sigma-Aldrich). The number of colonies that consisted of at least 50 cells was counted. The survival fraction (SF) was calculated to determine the ability of the Ishikawa cells to grow into colonies by the following equations. This method was based on that of Franken et al.<sup>22</sup>: plating efficiency (PE)=(No. of colonies formed/No. of cells seeded)×100% and SF=No. of colonies formed/(No. of cells seeded×PE).

#### Cell Cycle Analysis

A total of  $1.6 \times 10^5$  Ishikawa cells were seeded in 35-mm culture dishes for 24 h at 37°C in a humidified 5% CO<sub>2</sub> atmosphere. The cells were treated with cordycepin, cisplatin, and combinations of the two for 24 h. They were then harvested, washed with PBS, centrifuged at 200×*g* for 3 min, and fixed with 70% ethanol overnight at –20°C. After fixation, the cells were washed twice with PBS and centrifuged at 200×*g* for 3 min, resuspended in 400 µl of PBS with 50 µl of RNase (R6513; Sigma-Aldrich) added (1 mg/ml), and incubated at 37°C for 30 min. Then 50 µl of propidium iodide (PI) solution (400 µg/ml) (P4170; Sigma-Aldrich) was added to stain the treated cells for 30 min. Cell cycle analysis was done on an Applied Biosystems Attune flow cytometer (Waltham, MA, USA) after gating out doublets in the PI

area versus width. Cell fractions in different phases were analyzed using Modfit LT 5.0.

#### Using Annexin V-FITC/PI Staining to Detect Apoptosis

A total of  $1.6 \times 10^5$  Ishikawa cells were seeded in 35-mm culture dishes overnight followed by treatment with cordycepin, cisplatin, or a combination of the two. After 24 h of treatment, cells were harvested and resuspended, washed twice with PBS, and centrifuged at 200×*g* for 3 min. The cells were resuspended using 500 µl of the binding buffer provided with the apoptosis kit (556547; BD Biosciences, San Diego, CA, USA). A suspension of 100 µl of cells was stained by adding 5 µl of annexin V-FITC and 5 µl of PI for 15 min at room temperature, followed by analysis of cellular apoptosis using an Applied Biosystems Attune flow cytometer and the manufacturer's software.

#### Synergistic Testing

Combination index (CI) was used to investigate the synergistic effects between cordycepin and cisplatin against the proliferation of Ishikawa cells. CI was calculated using the Chou–Talalay CI method implemented in CompuSyn software<sup>23</sup>. This method incorporates several biochemistry and biophysics equations, such as the Henderson–Hasselbalch, Michaelis–Menten, and Scatchard equations. CI values allow quantitative indication of synergism (CI<1), antagonism (CI>1), and additive effect (CI=1) in drug combinations.

#### In Silico Molecular Docking Studies

Molecular docking simulations have been extensively used to predict the binding affinities of proteins and ligands. The technique has been successfully used to screen active compounds from herbal medicines with

pharmacological effects<sup>24</sup>. In our study, two similar docking procedures were performed on A<sub>3</sub>AR and ADA and their related ligands.

As noted above, cordycepin binds to and induces the activity of A<sub>3</sub>AR and exerts anticancer effects. Docking simulations can only predict the binding affinity between a protein and ligand; they cannot clarify whether the ligand is an inhibitor or agonist. Also, it is much more difficult to design a novel agonist than an inhibitor. Hence, to increase the success rate for identifying an A<sub>3</sub>AR agonist with low ADA metabolism, we downloaded 47 experimentally proven A<sub>3</sub>AR agonists with similar chemical structures to cordycepin from the International Union of Basic and Clinical Pharmacology (IUPHAR) database (<http://www.guidetopharmacology.org>). Five of these agonists are labeled with radioactive isotopes, and 11 have binding affinity values derived from nonhuman species. Hence, these 16 compounds were omitted, leaving 31 agonists for investigation in this study. IUPHAR contains curated information on quantitative interactions between 1,300 protein targets and 6,000 ligands<sup>25</sup>. Unlike other databases, it allows searches on agonists or antagonists of particular protein targets. No X-ray structure is currently available for human A<sub>3</sub>AR<sup>16</sup>, so we used the homology model template (PDB code: 2YDO, 3.00 Å resolution) downloaded from the Adenosiland platform (<http://mms.dsfarm.unipd.it/Adenosiland>)<sup>26</sup>. This structure has been used in various studies and has produced promising results<sup>27,28</sup>. For the dockings between the 31 compounds and ADA, the structure with PDB code 3IAR and 1.52 Å resolution was used. It is the only X-ray structure derived from *Homo sapiens*.

The automated ligand docking program, GOLD v5.5<sup>29</sup> with ChemPLP scoring function<sup>30</sup>, was used for all docking simulations. All water molecules, ligands, and ions were removed, and hydrogen was added before the docking simulations. All the parameters were set to their defaults. Genetic algorithms with 100% search efficiency, no possibility of early termination, and a slow option were used. Binding sites were defined as all atoms within 6 Å of the cognate ligands in the X-ray structures. In summary, cordycepin and its 31 structural related compounds were docked to both A<sub>3</sub>AR and ADA, with the aim of identifying an A<sub>3</sub>AR agonist with low ADA binding affinity.

#### Validation of the Docking Methods

ChemPLP@GOLD is an empirical scoring function that has been successfully validated on diverse sets of protein–ligand complexes. The genetic docking algorithm of GOLD has been tested on a data set of 100 complexes and achieved a 71% success rate in detecting experimental binding modes<sup>29</sup>. ChemPLP@GOLD achieved the highest success rates in a docking power test

and ranked fourth for scoring power among 20 different scoring functions on a dataset of 195 protein–ligand complexes<sup>31</sup>. However, research has shown that the accuracy of docking can vary between 0% and 92.66%<sup>32</sup>. This large variation chiefly depends on the type of protein–ligand complexes, docking algorithms, and scoring functions. The accuracy of a specific type of docking simulation should therefore always be validated. We evaluated the specific performance of ChemPLP@GOLD in simulating ADA and A<sub>3</sub>AR complexes using receiver operating characteristic (ROC) analysis.

To evaluate the accuracy of our docking procedures for ADA, docking was performed on 13,056 compounds from the Zinc in Man (ZIM) database<sup>33</sup>, plus 58 ADA inhibitors with experimental binding affinities of less than 10 µM. The 58 inhibitors classified as “ADA\_HUMAN” were downloaded from the ZINC database. In total, a set of 13,114 compounds was formed, and each compound was docked to ADA under our docking protocol. The docking scores were then used as the parameters in the ROC analysis to calculate area under the curve (AUC) values, which demonstrate the ability of ChemPLP@GOLD to distinguish the 58 “true” hits from the 13,056 non-ADA inhibitors. ROC analysis has successfully validated docking accuracy in various protein–ligand systems<sup>34,35</sup>.

For the accuracy evaluation of our docking procedures on A<sub>3</sub>AR, ROC analysis was performed on a library of 13,087, containing the 13,056 compounds from the ZIM database<sup>33</sup> and the 31 A<sub>3</sub>AR agonists from the ZINC database using the same docking protocol as mentioned above.

#### Prediction of Drug-Like Properties

The undesired adverse effects of drug candidates are among the most common reasons for the failure of animal or clinical trials. Screening of drug-like properties can help to identify potential drug candidates with unacceptable adverse effects. For reliable prediction, two different software programs—ACD/Percepta 14.0<sup>36</sup> and Drug-Likeness and Molecular Property Prediction<sup>37</sup>—were used in this study to predict the drug-like properties and drug-likeness of all 31 A<sub>3</sub>AR inducers.

The drug profiler of ACD/Percepta 14.0 was used to predict the physicochemical properties, ADME (adsorption, distribution, metabolism, excretion), and drug safety profile of the 31 compounds. The physicochemical properties included log P, molecular weight (MW), solubility, rotatable bond, H-bond receptors, H-bond donors, Lipinski's rule of five, and predefined lead-like categories. This software automatically shows whether compounds have favorable or unfavorable physicochemical properties for a drug molecule. The ADME profiler predicts the parameters that are important for oral bioavailability. These parameters are plasma protein binding

**Table 2.** IC<sub>50</sub> Values for Cordycepin, Cisplatin, and Their Combinations on Ishikawa Cells

Compounds (Concentration)	IC <sub>50</sub> (µg/ml)
Cordycepin	86.16
Cisplatin	3.74
Cisplatin plus cordycepin (12.5 µg/ml)	2.53
Cisplatin plus cordycepin (25 µg/ml)	2.29

(PPB), passive permeability across Caco-2 cell monolayers, central nervous system (CNS) penetration, and human intestinal absorption (HIA). The drug safety profiler predicts cytochrome P450 (CYP) regioselectivity (CYP3A4, CYP2D6, CYP2C9, CYP2C19, and CYP1A2), and the possibility of producing positive Ames (mutagenicity prediction) and human ether-a-go-go-related gene (hERG) (cardiotoxicity prediction)<sup>38,39</sup>. The accuracy and sensitivity of these methods have been successfully validated by the software providers (ACD/Labs). All data sheets can be obtained from its website (<http://www.acdlabs.com>).

Drug-Likeness and Molecular Property Prediction is an online platform for the use of fragment-based contributions to calculate drug-like properties, such as LogP, LogS, molecular polar surface area, and drug-likeness score. The accuracy of its methods has been successfully validated with a large amount of experimental data, and results obtained from this software have been published in many studies<sup>40,41</sup>.

## RESULTS

### *Inhibition of Ishikawa Cells*

The effects of cordycepin, cisplatin, and their combination on the inhibition of Ishikawa cell lines were observed

by MTT assay. Dose-dependent inhibitory effects were found for both compounds. As shown in Table 1, 100 µg/ml of cordycepin solution produced comparable inhibition effects to cisplatin at 4 µg/ml. Compared with cisplatin alone, the combined use of 12.5 µg/ml of cordycepin and 4 µg/ml of cisplatin increased the inhibition rate from 51.6% to 76.8% (Table 1). The combination of cisplatin with cordycepin obtained lower IC<sub>50</sub> values than cordycepin or cisplatin alone (Table 2). Cordycepin demonstrated synergistic effects in combination with cisplatin, as indicated by a CI value of 0.811. This demonstrates the potential for the adjunctive use of cordycepin with cisplatin.

### *Clonogenic Survival Assay*

In order to observe the effects of cordycepin, cisplatin, and their combinations on the clone ability of Ishikawa cells, clonogenic survival assays were performed. Both compounds and their combinations inhibited Ishikawa cell clone formation with dose-dependent effects (Table 3). Cordycepin solution with a concentration of 100 µg/ml produced similar effects to cisplatin at 0.5 µg/ml. The combined use of cordycepin and cisplatin decreased the SF of cisplatin or cordycepin alone; for instance, the SF of cordycepin solution at 12.5 µg/ml was 0.97, that of cisplatin solution at 0.0625 µg/ml was 0.51, and that of the combined solution of cisplatin cordycepin at 12.5 and 0.0625 µg/ml was 0.34 (Table 3). This indicates that the combinations have greater potential to inhibit the formation of clone than each of them alone.

### *Cellular Apoptosis of Ishikawa Cells*

To investigate whether cordycepin, cisplatin, and their combination could induce cellular apoptosis, Ishikawa cells stained with annexin V-FITC/PI were examined by

**Table 3.** Survival Fraction on Ishikawa Cells of Cordycepin, Cisplatin, and Their Combinations

Compounds (Concentration)	Survival Fraction*
Cordycepin (12.5 µg/ml)	0.97±0.02
Cordycepin (25 µg/ml)	0.78±0.01
Cordycepin (50 µg/ml)	0.15±0.03
Cordycepin (100 µg/ml)	0.02±0.02
Cisplatin (0.0625 µg/ml)	0.51±0.03
Cisplatin (0.125 µg/ml)	0.36±0.03
Cisplatin (0.25 µg/ml)	0.06±0.01
Cisplatin (0.5 µg/ml)	0.02±0.01
Cordycepin (12.5 µg/ml) plus cisplatin (0.0625 µg/ml)	0.34±0.04
Cordycepin (12.5 µg/ml) plus cisplatin (0.125 µg/ml)	0.24±0.01
Cordycepin (12.5 µg/ml) plus cisplatin (0.25 µg/ml)	0.04±0.01
Cordycepin (25 µg/ml) plus cisplatin (0.0625 µg/ml)	0.34±0.04
Cordycepin (25 µg/ml) plus cisplatin (0.125 µg/ml)	0.18±0.01
Cordycepin (25 µg/ml) plus cisplatin (0.25 µg/ml)	0.02±0.01

\*The values of all survival fractions are  $p < 0.01$ .

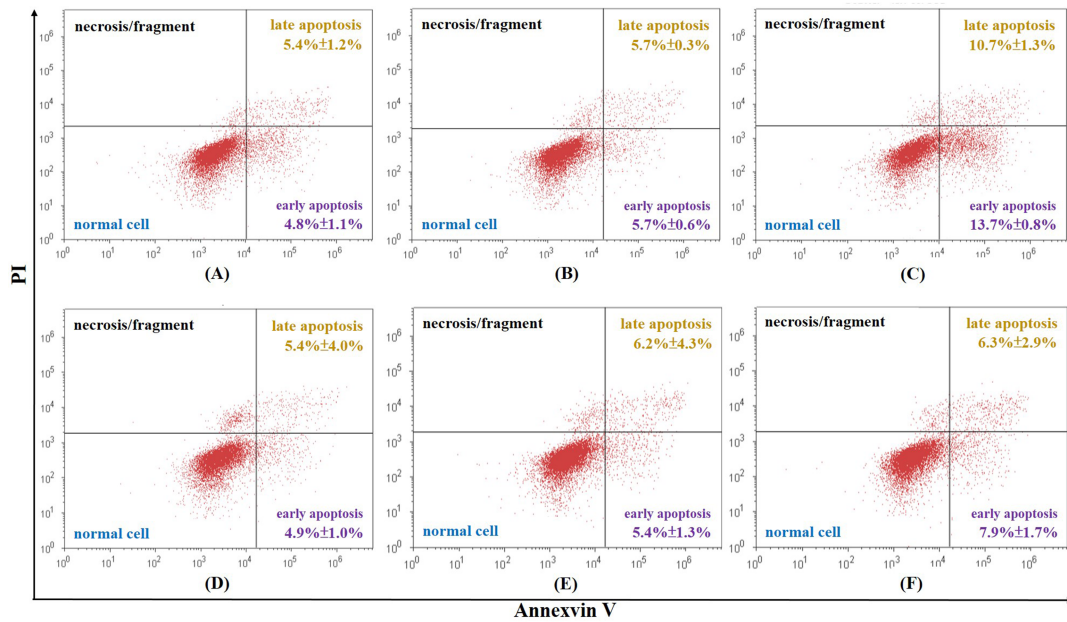


**Figure 1.** Total rate of cellular apoptosis of Ishikawa cells caused by (A) 12.5 µg/ml of cordycepin is  $10.2\% \pm 2.2\%$ , (B) 25 µg/ml of cordycepin is  $11.4\% \pm 0.2\%$ , (C) 50 µg/ml of cordycepin is  $24.4\% \pm 1.6\%$ , (D) 0.5 µg/ml of cisplatin is  $10.3\% \pm 3.3\%$ , (E) 1 µg/ml of cisplatin is  $11.6\% \pm 5.6\%$ , and (F) 2 µg/ml of cisplatin is  $14.2\% \pm 4.2\%$ .

flow cytometry. The total rate of apoptosis of the control is  $6.3\% \pm 1.4\%$ . All samples achieved a higher rate of apoptosis than the control samples in a dose-dependent manner. Most of the differences were statistically significant, apart from cordycepin at 12.5 µg/ml, cisplatin at

0.5 µg/ml, cisplatin at 1 µg/ml, and cordycepin plus cisplatin at 12.5 and 0.5 µg/ml, respectively, which had no statistically different effect on cellular apoptosis compared to the control group ( $p > 0.05$ ) (Figs. 1 and 2). Among all the samples, the highest concentration of cordycepin plus

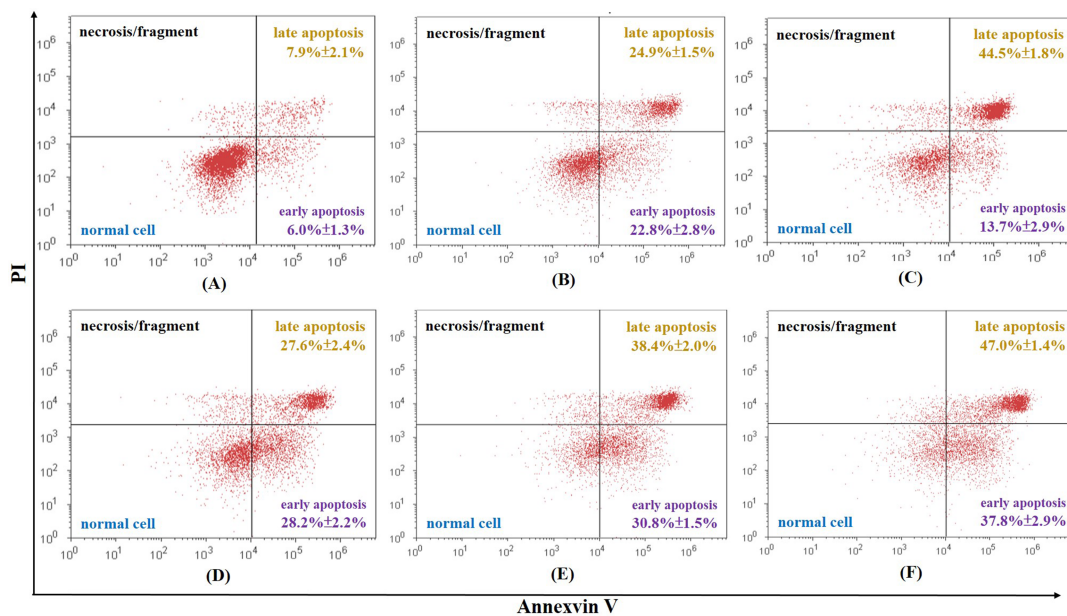


**Figure 2.** Total rate of cellular apoptosis of Ishikawa cells caused by (A) 12.5 µg/ml of cordycepin + 0.5 µg/ml cisplatin is  $13.9\% \pm 1.4\%$ , (B) 12.5 µg/ml of cordycepin + 1 µg/ml cisplatin is  $47.7\% \pm 1.6\%$ , (C) 12.5 µg/ml of cordycepin + 2 µg/ml cisplatin is  $58.2\% \pm 4.6\%$ , (D) 25 µg/ml of cordycepin + 0.5 µg/ml cisplatin is  $55.8\% \pm 2.7\%$ , (E) 25 µg/ml of cordycepin + 1 µg/ml cisplatin is  $69.2\% \pm 3.1\%$ , and (F) 25 µg/ml of cordycepin + 2 µg/ml cisplatin is  $84.8\% \pm 4.2\%$ .

**Table 4.** Effects of Cordycepin, Cisplatin, and Their Combinations on Ishikawa Cell Cycle

Compounds (Concentration)	G <sub>0</sub> /G <sub>1</sub>	S	G <sub>2</sub>
Control	42.4% ± 2.3%	46.3% ± 3.6%	11.4% ± 1.5%
Cordycepin (12.5 µg/ml)	57.9% ± 3.4%	29.4% ± 1.1%	12.9% ± 2.9%
Cordycepin (25 µg/ml)	57.6% ± 3.6%	31.1% ± 3.5%	11.5% ± 2.7%
Cisplatin (0.5 µg/ml)	11.1% ± 0.1%	63.2% ± 1.4%	25.7% ± 1.4%
Cisplatin (1 µg/ml)	5.1% ± 2.4%	72.4% ± 2.5%	22.6% ± 4.9%
Cisplatin (2 µg/ml)	4.9% ± 4.4%	80.5% ± 1.2%	14.6% ± 3.3%
Cordycepin (12.5 µg/ml) plus cisplatin (0.5 µg/ml)	10.7% ± 1.5%	77.9% ± 4.3%	11.5% ± 5.7%
Cordycepin (12.5 µg/ml) plus cisplatin (1 µg/ml)	7.5% ± 3.5%	80.7% ± 2.2%	11.8% ± 4.4%
Cordycepin (25 µg/ml) plus cisplatin (0.5 µg/ml)	13.5% ± 0.7%	71.4% ± 2.6%	15.1% ± 2.2%
Cordycepin (25 µg/ml) plus cisplatin (1 µg/ml)	14.5% ± 0.7%	82.7% ± 1.7%	2.8% ± 1.9%

cisplatin (25 µg/ml+2 µg/ml) obtained the highest rate of apoptosis (84.8%) (Fig. 2). However, a low concentration of cordycepin plus cisplatin (12.5 µg/ml+0.5 µg/ml) did not produce a more significant increase in the rate of apoptosis than cisplatin (0.5 µg/ml) alone (Fig. 2).

#### Effects of Cordycepin and Cisplatin on the Cell Cycle

To determine the effects of cordycepin and/or cisplatin on the cell cycle distribution in Ishikawa cells, we performed flow cytometry with PI staining. The results show that cordycepin significantly increased the percentage of G<sub>0</sub>/G<sub>1</sub> phase and decreased the percentage of S phase cells (Table 4 and Fig. 3). Cisplatin significantly arrested Ishikawa cells in the S phase, and the percentage of G<sub>2</sub> phase cells was slightly increased (Table 4 and Fig. 3). After the combined treatment, the arrest effects of cisplatin in the S phase of the Ishikawa cell cycle were

enhanced by cordycepin (Table 4 and Fig. 4). The percentage of S phase cells after cisplatin treatment (0.5 µg/ml) was 63.2%, and those of cisplatin (0.5 µg/ml) plus cordycepin (12.5 µg/ml and 25 µg/ml) were 77.9% and 71.4%, respectively. Cisplatin (1 µg/ml) arrested 72.4% of Ishikawa cells in the S phase, whereas cisplatin (1 µg/ml) plus cordycepin (12.5 and 25 µg/ml) arrested 80.7% and 82.7% of Ishikawa cells in the S phase, respectively (Table 4 and Fig. 4).

#### Validation of the Docking Methods

The accuracy of our docking protocols for both ADA and A<sub>3</sub>AR was successfully validated using the ROC analysis (Fig. 5). The high AUC values of 0.92 (ADA) and 0.85 (A<sub>3</sub>AR) indicate satisfactory predictive power with high sensitivity and specificity. An AUC value of 0.5 indicates a random result with no predictive power, and 1.0

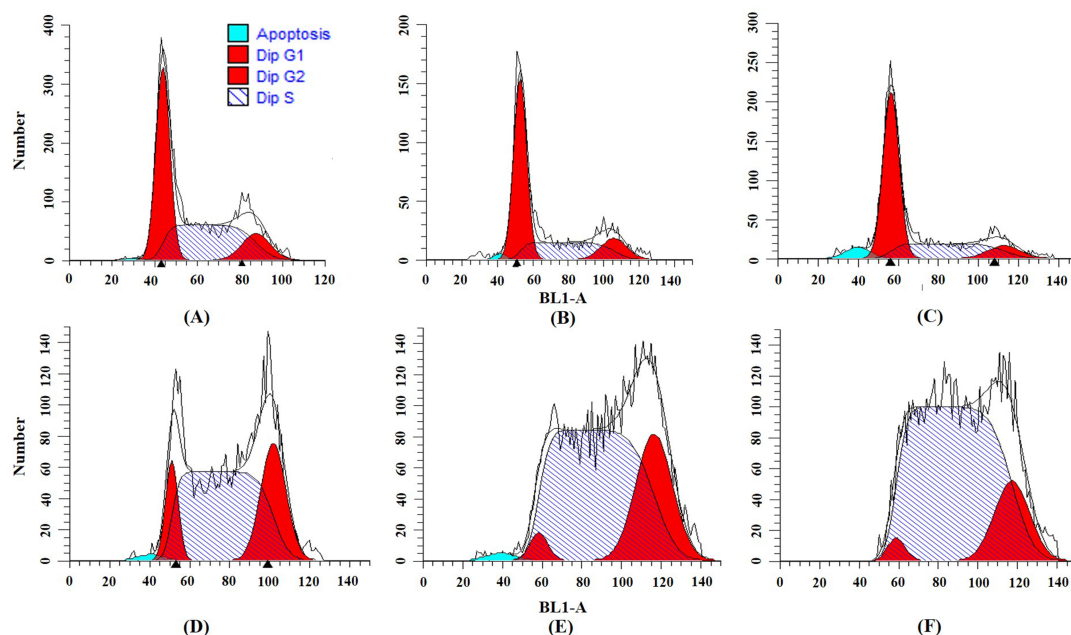


**Figure 3.** Effects on the Ishikawa cell cycle caused by (A) control, (B) 12.5 µg/ml of cordycepin, (C) 25 µg/ml of cordycepin, (D) 0.5 µg/ml of cisplatin, (E) 1 µg/ml of cisplatin, and (F) 2 µg/ml of cisplatin.

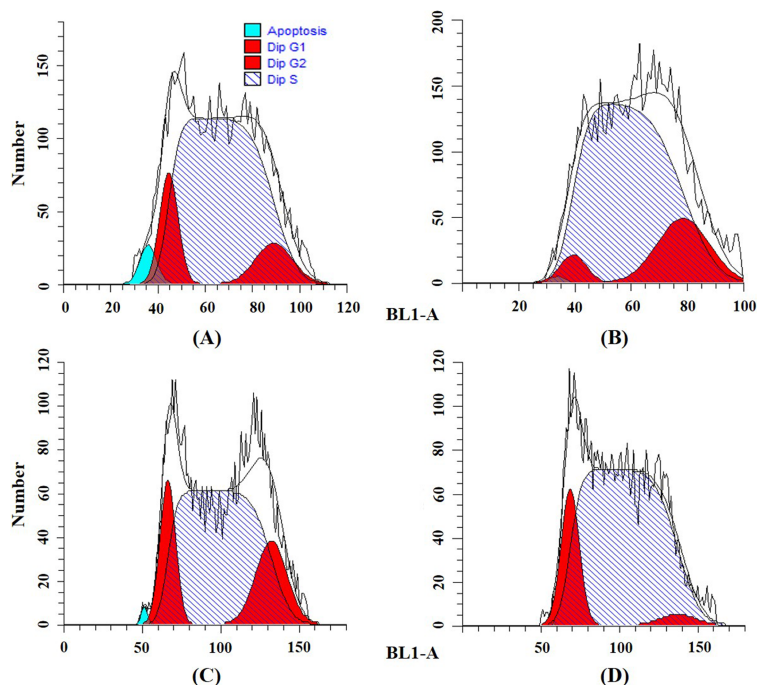


**Figure 4.** Effects on Ishikawa cell cycle caused by (A) 12.5 µg/ml cordycepin+0.5 µg/ml cisplatin, (B) 12.5 µg/ml cordycepin+1 µg/ml cisplatin, (C) 25 µg/ml cordycepin+0.5 µg/ml cisplatin, and (D) 25 µg/ml cordycepin+1 µg/ml cisplatin.

indicates a perfect prediction. A model with an AUC value of 0.7 or above is generally considered reliable<sup>35</sup>.

#### *In Silico Molecular Docking Studies*

Thirty of the 31 A<sub>3</sub>AR agonists achieved a higher binding score than cordycepin (Table 5). CGS21680 and apadenoson obtained the highest scores of 108.69 and 103.78, respectively. In the ADA docking simulations, 15 of the 31 agonists had a lower score than cordycepin. Among them, MRS5698 obtained the lowest score

of 30.58, which is half the value of that of cordycepin (Table 5). The agonist with the second-lowest docking score against ADA was 2-chloroadenosine. Its score was 46.89, which is much higher than that of MRS5698. The structures of cordycepin, 2-chloroadenosine, and MRS5698 are shown in Figure 6.

#### *Prediction of Drug-Like Properties*

All 31 agonists had Caco-2 values of less than 1, indicating poor passive intestinal permeability (Table 5).

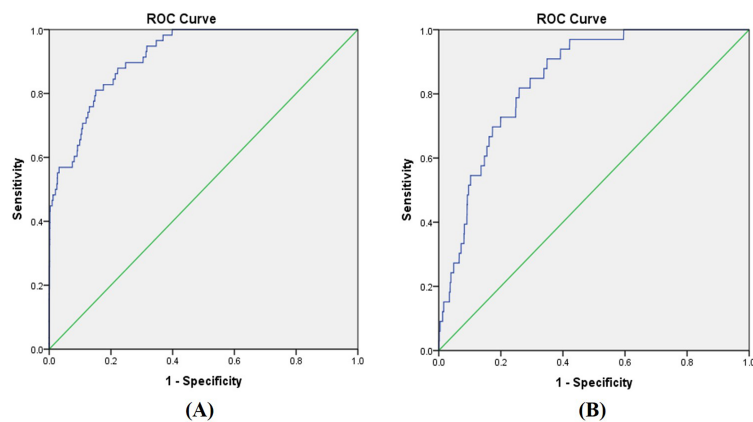


**Figure 5.** Receiver operating characteristic (ROC) curves of the docking results for (A) ADA and the ligands from the ZIM database, and (B) A<sub>3</sub>AR and the ligands from the ZIM database. The green reference line indicates random results, with an AUC value of 0.50. The blue line indicates the result curve with AUC values of (A) 0.92 and (B) 0.85. AUC, area under the curve; ADA, adenosine deaminase; A<sub>3</sub>ARs, A<sub>3</sub> adenosine receptors; ZIM, Zinc in Man.



**Table 5.** Docking Scores and ADME Drug-Like Properties of Cordycepin and the 31 A<sub>3</sub>AR Agonists Against ADA and A<sub>3</sub>AR

Ligand	Caco-2	PPB (%)	CNS	HIA (%)	Docking Score	
					ADA	A <sub>3</sub> AR
Cordycepin	2×10 <sup>-6</sup>	2	-3.21	69	64.74	61.65
MRS5698	94×10 <sup>-6</sup>	76	-2.74	100	30.58	69.41
2-Chloroadenosine	0.7×10 <sup>-6</sup>	6	-3.50	46	46.89	66.95
2'-Me-CCPA	33×10 <sup>-6</sup>	19	-2.75	100	47.91	72.08
TCPA	0.1×10 <sup>-6</sup>	52	-5.70	4	48.24	62.85
NECA	0.4×10 <sup>-6</sup>	3	-4.28	31	50.04	74.43
MRE3008F20	11×10 <sup>-6</sup>	97	-5.08	100	52.32	54.42
2-Phenylethyl-adenosine derivative	12×10 <sup>-6</sup>	47	-3.43	100	52.91	86.20
Adenosine	0.4×10 <sup>-6</sup>	2	-3.72	30	55.21	64.63
GS9667	19×10 <sup>-6</sup>	13	-2.93	100	57.20	79.72
Binodenoson	0.6×10 <sup>-6</sup>	9	-4.13	34	58.36	84.77
( <i>R,S</i> )-PHPNECA	0.7×10 <sup>-6</sup>	6	-3.50	46	59.86	86.73
<i>N</i> (6)-cyclohexyladenosine	16×10 <sup>-6</sup>	10	-2.48	100	61.76	69.34
HEMADO	19×10 <sup>-6</sup>	13	-2.93	100	63.38	75.65
CI-IB-MECA	54×10 <sup>-6</sup>	63	-2.98	100	64.08	82.17
Regadenoson	0.0×10 <sup>-6</sup>	2	-5.30	6	64.31	80.15
Piclidenoson	26×10 <sup>-6</sup>	29	-3.01	100	65.25	79.16
Cyclopentyladenosine	10×10 <sup>-6</sup>	6	-2.66	100	65.85	68.79
PENECA	3×10 <sup>-6</sup>	34	-3.75	92	66.75	87.18
BAY606583	59×10 <sup>-6</sup>	81	-2.92	100	67.84	82.66
AB-MECA	2×10 <sup>-6</sup>	6	-3.14	84	70.23	73.67
MPC-MECA	9×10 <sup>-6</sup>	24	-3.48	100	70.63	76.48
MRS3558	31×10 <sup>-6</sup>	52	-3.00	100	73.87	91.86
2-Hexynyl-NECA	2×10 <sup>-6</sup>	13	-3.68	89	73.91	93.66
Apadenoson	5×10 <sup>-6</sup>	22	-3.70	98	75.72	103.78
CCPA	26×10 <sup>-6</sup>	19	-2.35	100	76.71	74.97
( <i>S</i> )-PIA	35×10 <sup>-6</sup>	13	-2.19	100	77.12	80.90
CP608,039	35×10 <sup>-6</sup>	13	-2.19	100	77.80	80.02
CGS21680	0.0×10 <sup>-6</sup>	45	-6.03	1	78.86	108.69
MRS5151	0.4×10 <sup>-6</sup>	3	-4.28	31	79.06	98.80
I-ABA	16×10 <sup>-6</sup>	10	-2.48	100	80.09	81.03
( <i>R</i> )-PIA	35×10 <sup>-6</sup>	13	-2.19	100	81.03	80.12

Caco-2 predicts passive intestinal permeability with the unit cm/s (>7.00 is highly permeable, 1.00–7.00 is moderately permeable, ≤1.00 is poorly permeable). Plasma protein binding (PPB) estimates the overall percentage bound in blood plasma protein. Central nervous system (CNS) values of ≤-3.50 indicate nonpenetrant to CNS; -3.50 to -3.00, weak penetrant; and >-3.00, penetrant. Human intestinal absorption (HIA) values of >70% are highly absorbed; 30%–70%, moderately absorbed; and ≤30%, poorly absorbed.

PPB varied significantly among the agonists, ranging from 2% to 97% (Table 5). Thirteen of the 31 agonists are CNS penetrant and may produce beneficial or detrimental pharmacological effects on the human CNS. Twenty-two agonists are considered to have high HIA, six have moderate absorption, and three have poor absorption (Table 5).

The physicochemical drug-like properties varied among the 31 agonists. Twenty had optimal Lipinski violation, and 14 had optimal lead-like violation (Table 6). All the agonists are predicted as either undefined or non-inhibitors of the five common cytochrome P450 enzymes involved in drug–drug interactions (Table 7). Undefined means the agonist obtained a borderline score between

inhibitor and noninhibitor. Hence, the chance of obtaining a correct prediction is low. The predictions of the Ames test classify all 31 agonists as undefined mutagenic (Table 7). Two of the agonists are predicted to be noninhibitors of the hERG channel; the others are undefined.

## DISCUSSION

Cisplatin is a well-known antitumor agent with numerous side effects. Its efficacy in endometrial cancer treatment is reducing due to drug resistance<sup>42</sup>. Therefore, a novel treatment replacing cisplatin or an adjuvant therapy for reducing its dosage is required. Cordycepin is a bioactive constituent of *C. sinensis*, which has been reported

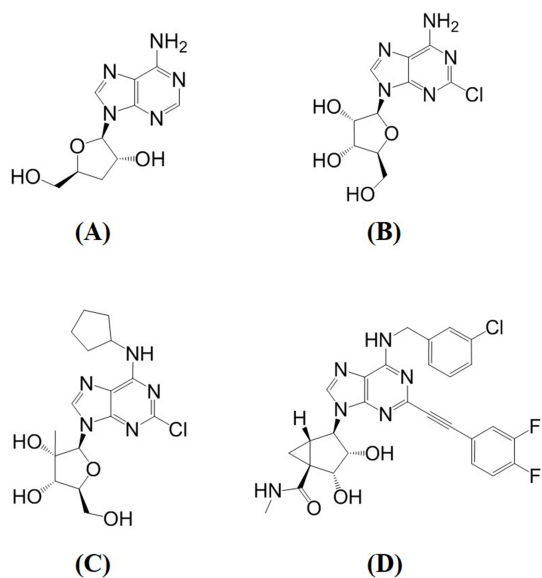


**Figure 6.** Structures of (A) cordycepin, (B) 2-chloroadenosine, (C) 2'-Me-CCPA, and (D) MRS5698.

as a potential compound against liver cancer, pancreatic cancer, and breast cancer because it induces cellular apoptosis and regulates the cell cycle<sup>7,9</sup>. This study is the first to determine that cordycepin can inhibit the proliferation of endometrial cancer cells and induce cellular apoptosis. Furthermore, a combination of cordycepin and cisplatin has a greater potential against endometrial cancer than cisplatin alone. The data from cytotoxicity and clonogenic assays show that combinations of cordycepin and cisplatin had higher inhibition rates and lower SF than those of the single compounds (Tables 1 and 3). The  $IC_{50}$  values were lowest in the combinations, followed by cisplatin and cordycepin (Table 2). The CI demonstrated synergistic effects of the two compounds. This study provides evidence that cordycepin can enhance the inhibitory effect of cisplatin on Ishikawa cells.

The cellular apoptosis analysis confirmed that cordycepin could induce cellular apoptosis in Ishikawa cells in a significant dose-dependent manner. The rate of apoptosis was positively correlated with inhibition rate with an excellent correlation coefficient of  $R^2 > 0.9$ , indicating that cordycepin inhibits the proliferation of Ishikawa cells by inducing cellular apoptosis. The cytotoxicity assay showed cisplatin's inhibition of the proliferation of Ishikawa cells with efficacious  $IC_{50}$  values of 3.74  $\mu\text{g}/\text{ml}$  for cancer treatment. However, the results of the cellular apoptosis investigations showed its rate of apoptosis was low (Figs. 1 and 2), which indicates that the ability to inhibit Ishikawa cell growth does not come from induced cellular apoptosis. Thus, cordycepin and cisplatin may have different pharmaceutical mechanisms, and combining them may produce advanced inhibition of

endometrial cancer cells. The rates of apoptosis of the combinations were positively correlated with the inhibition rates ( $R^2 > 0.9$ ).

To further investigate the effect of cordycepin on Ishikawa cells, cell cycle analysis with flow cytometry was used. The results show that cordycepin can arrest cells in the  $G_0/G_1$  phase (Table 4), which means that cordycepin has the potential to interfere with the expression of mRNA and affect DNA synthesis. Hence, cells will not be able to proliferate DNA and enter the S phase, and eventually cellular apoptosis and cell death will result. Unlike cordycepin, cisplatin can arrest Ishikawa cells in the S phase (Table 4) and potentially interfere with DNA synthesis. This means that cisplatin somehow inhibits the proliferation of Ishikawa cells by regulating the cell cycle. The combinations of cordycepin and cisplatin achieved the best results in the cytotoxicity assays, cellular apoptosis analysis, and cell cycle analysis. Thus, further *in vivo* or animal synergistic studies on the combined use of cordycepin and cisplatin would be of value.

A review of previous studies has demonstrated the rapid metabolism of cordycepin by ADA<sup>19</sup>. This may affect the bioavailability and, hence, the effectiveness of cordycepin in clinical use. We therefore performed computational docking simulations on 31 cordycepin derivatives, aiming to preserve the antitumor activity of cordycepin but with lowered metabolism by ADA.

The resulting docking scores reveal that most of the  $A_3AR$  agonists bind to  $A_3AR$  more stably than cordycepin does. These agonists were developed based on the chemical structure of cordycepin, and most of them have been shown to have high binding affinities against  $A_3AR$ <sup>16</sup>. Our results align with the literature and further endorse the assertion that these agonists have similar binding affinities to cordycepin. This  $A_3AR$  binding is the main pharmacological mechanism of the antitumor effects of cordycepin<sup>18</sup>.

Of the 31 agonists, CGS21680 and apadenoson achieved the most favorable binding to  $A_3AR$ , as indicated by the highest docking score (Table 5). This suggests that both agonists may have antitumor effects that are similar to or better than those of cordycepin. However, their docking scores against ADA were 78.86 and 75.72, which are higher than that of cordycepin (Table 5). ADA is responsible for the rapid metabolism of cordycepin. Hence, both CGS21680 and apadenoson will also be rapidly metabolized by ADA and could not exert the required antitumor activities.

In the docking simulations of ADA, half of the 31 agonists bound less favorably than cordycepin. This indicates that half of them may be metabolized less rapidly than cordycepin. Among these agonists, the binding affinity of MRS5698 was less than half that of cordycepin (Table 5). This indicates that the additional functional

**Table 6.** Physicochemical Drug-Like Properties of the 31 A<sub>3</sub>AR Agonists

Ligand	LogP	MW	H-Bond Donors	H-Bond Acceptors	Rotatable Bonds	Rings	Lipinski	Lead-Like	Aqueous Solubility
MRS5698	3.09	565.0	4	9	7	6	1	1	0.007
2-Chloroadenosine	-0.47	301.7	5	9	2	3	0	0	0.55
2'-Me-CCPA	1.87	383.8	4	9	4	4	0	0	0.27
TCPA	1.09	497.5	6	14	7	6	2	3	0.52
NECA	-0.83	308.3	5	10	3	3	0	1	19.1
MRE3008F20	2.26	423.4	2	11	6	5	1	1	0.38
2-Phenylethyl-adenosine derivative	1.1	408.4	4	10	5	4	0	1	0.35
Adenosine	-0.98	267.2	5	9	2	3	0	0	1.62
GS9667	1.44	361.4	4	9	7	3	0	0	0.08
Binodenson	0.33	391.4	6	11	5	4	2	2	0.39
( <i>R,S</i> )-PHPNECA	-0.47	301.7	5	9	2	3	0	0	0.55
<i>N</i> (6)-cyclohexyladenosine	1.29	349.4	4	9	4	4	0	0	0.73
HEMADO	1.44	361.4	4	9	7	3	0	0	0.08
Cl-IB-MECA	2.36	544.7	4	10	5	4	1	2	0.1
Regadenoson	-1.82	390.4	6	13	4	4	2	2	5.27
Piclidenoson	1.69	510.3	4	10	5	4	1	2	0.56
Cyclopentyladenosine	0.88	355.4	4	9	4	4	0	0	1.19
PENECA	0.66	408.4	5	10	5	4	0	1	0.19
BAY60-6583	2.43	379.4	4	7	9	3	0	0	0.004
AB-MECA	0.98	498.3	6	10	5	4	1	3	0.29
MPC-MECA	0.91	428.3	4	11	7	4	1	1	2.52
MRS3558	1.86	463.3	4	9	5	5	0	1	0.05
2-Hexynyl-NECA	0.56	388.4	5	10	7	3	0	1	0.23
Apadenoson	1.08	486.5	5	12	8	4	1	2	0.21
CCPA	1.65	369.8	4	9	4	4	0	0	0.28
( <i>S</i> )-PIA	1.95	385.4	4	9	6	4	0	0	0.09
CP608,039	1.95	385.4	4	9	6	4	0	0	0.09
CGS21680	0.69	499.5	7	13	10	4	2	3	15.1
MRS5151	-0.83	308.3	5	10	3	3	0	1	19.1
I-ABA	1.29	349.4	4	9	4	4	0	0	0.73
( <i>R</i> )-PIA	1.95	385.4	4	9	6	4	0	0	0.09

Log P represents octanol–water partition coefficient under standard conditions at 25°C (values for optimal drug-like properties are -1.00 to 4.20). MW indicates molecular weight (optimal values are ≤460.00). Optimal numbers of H-bond donors, H-bond acceptors, rotatable bonds, and rings are ≤5, ≤10, ≤10, and <4, respectively. Optimal numbers of violations for both Lipinski and lead-like are <1. Aqueous solubility was calculated at pH 6.4 and in mg/ml (≤0.01 indicates highly insoluble; 0.01–0.1, insoluble; and >0.1, soluble).

groups of MRS5698 related to cordycepin are somehow unfavorable to binding with ADA. Through careful analysis of the binding mode of MRS5698, we noticed that several hydrogen atoms of MRS5698 and the binding site residues of ADA are located very close to each other (Fig. 7A). This may produce repulsive interactions between MRS5698 and ADA. In the binding of cordycepin and ADA, these hydrogen interactions are absent (Fig. 7B), although MRS5698 is predicted to have a similar binding affinity to cordycepin (Table 5). This indicates that MRS5698 can bind to A<sub>3</sub>AR and attenuate cancer cell growth, but with less metabolism by ADA.

Studies show that MRS5698 is highly selective to human and mouse A<sub>3</sub>AR, as indicated by a  $K_i$  value of 3 nM<sup>43</sup>. Its binding to A<sub>3</sub>AR is about 1,000 times stronger than that of the structurally similar subtypes of adenosine

receptors, A<sub>1</sub>AR and A<sub>2</sub>AR<sup>44</sup>. Paoletta et al.<sup>45</sup> also reported the high selectivity of MRS5698 in more than 50 other cell surface receptors and ion channels. This high specificity lessens the possibility of adverse side effects resulting from binding to other receptors.

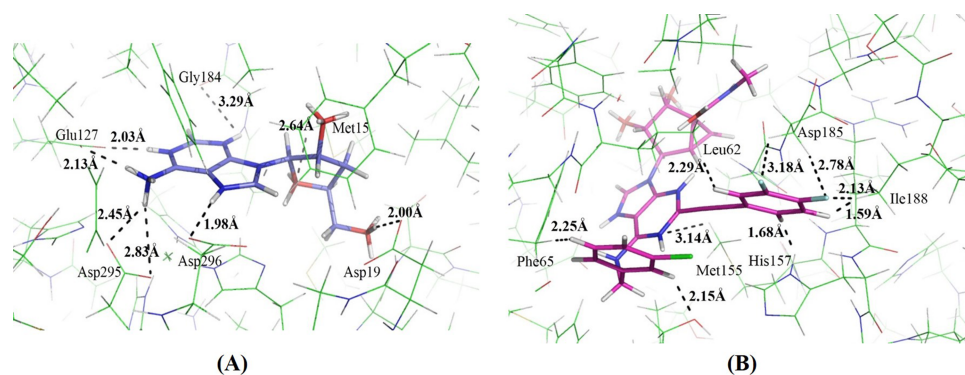
MRS5698 is predicted to be a penetrant of the CNS, as indicated by its CNS value of less than -3.00 (Table 5). This indicates the possibility of producing biological effects in the human CNS, which can be beneficial or detrimental. MRS5698 has been shown to cross the blood–brain barrier<sup>46</sup> and possibly produce neuroprotective effects with a similar mechanism to cordycepin<sup>47</sup>. Certainly, further investigations of these potentially therapeutic effects are required.

In our study, MRS5698 obtained an HIA value of 100% (Table 5), which indicates that it can be effectively

**Table 7.** Drug Safety of the 31 A<sub>3</sub>AR Agonists

Ligand	Ames	hERG	CYP1A2	CYP2C9	CYP2C19	CYP2D6	CYP3A4
MRS5698	0.43	0.40	U	U	U	U	U
2-Chloroadenosine	0.42	0.36	NI	NI	NI	NI	NI
2'-Me-CCPA	0.44	0.41	NI	NI	NI	NI	NI
TCPA	0.47	0.42	NI	NI	U	NI	NI
NECA	0.56	0.31	NI	NI	NI	NI	NI
MRE 3008F20	0.48	0.46	U	U	U	U	U
2-Phenylethyl-adenosine derivative	0.43	0.39	NI	NI	NI	NI	U
Adenosine	0.47	0.37	NI	NI	NI	NI	NI
GS9667	0.42	0.37	NI	NI	NI	NI	NI
Binodenoson	0.46	0.42	NI	NI	NI	NI	NI
( <i>R,S</i> )-PHPNECA	0.42	0.36	NI	NI	NI	NI	NI
<i>N</i> (6)-cyclohexyladenosine	0.39	0.41	NI	NI	NI	NI	NI
HEMADO	0.42	0.37	NI	NI	NI	NI	NI
Cl-IB-MECA	0.42	0.38	NI	U	U	NI	NI
Regadenoson	0.48	0.37	NI	NI	NI	NI	NI
Piclidenoson	0.46	0.37	NI	NI	U	NI	NI
Cyclopentyladenosine	0.4	0.42	NI	NI	NI	NI	NI
PENECA	0.48	0.41	NI	NI	NI	NI	U
BAY60-6583	0.55	0.47	U	U	U	U	U
AB-MECA	0.47	0.4	NI	NI	NI	NI	NI
MPC-MECA	0.47	0.41	NI	NI	NI	NI	U
MRS3558	0.46	0.4	NI	U	U	NI	U
2-Hexynyl-NECA	0.49	0.34	NI	NI	NI	NI	U
Apadenoson	0.39	0.34	NI	NI	NI	NI	U
CCPA	0.43	0.4	NI	NI	NI	NI	NI
( <i>S</i> )-PIA	0.38	0.35	NI	NI	NI	NI	NI
CP608,039	0.38	0.35	NI	NI	NI	NI	NI
CGS21680	0.42	0.45	NI	NI	NI	NI	NI
MRS5151	0.56	0.31	NI	NI	NI	NI	NI
I-ABA	0.39	0.41	NI	NI	NI	NI	NI
( <i>R</i> )-PIA	0.38	0.35	NI	NI	NI	NI	NI

CYP, cytochrome P450; NI, noninhibitor; U, undefined. Ames test estimates mutagenic potential ( $\leq 0.33$  indicates nonmutagenic; 0.33–0.67, undefined; and  $>0.67$ , mutagenic). hERG predicts interaction potential with the hERG channel, which may cause cardiotoxicity ( $\leq 0.33$  indicates noninhibitor; 0.33–0.67, undefined; and  $>0.67$ , inhibitor).

**Figure 7.** Binding mode of (A) MRS5698 and (B) cordycepin in ADA active site.

absorbed by the human intestine. However, it obtained a poor Caco-2 value in both this study (Table 5) and that of Tosh et al.<sup>43</sup>, suggesting the intestinal efflux of MRS5698, which may affect its total absorption in humans. Nevertheless, MRS5698 has already demonstrated good oral absorption and was highly efficacious in animal studies when administered orally<sup>43</sup>. With regard to PPB, MRS5698 is predicted to have a value of 76%. In general, a PPB value of more than 80% indicates some clinical concern<sup>48</sup> because large amounts of the drug may bind to plasma protein with only a small proportion reaching the target. Moreover, high PPB values also indicate a higher chance of drug–drug interactions via competing plasma proteins. Nevertheless, some commonly used drugs such as dicloxacillin and flucloxacillin have PPB values of greater than 90%<sup>49</sup>.

In terms of the drug safety profile, MRS5698 was predicted to be “undefined” for all five CYP isoforms (Table 7); that is, it obtained a borderline score between inhibitor and noninhibitor. This agrees with the in vitro ADME studies performed by Tosh et al.<sup>43</sup>, in which MRS5698 exhibited no or poor inhibitory activities against the three major CYP isoforms CYP2C9 (47  $\mu$ M), CYP2C19 (22  $\mu$ M), and CYP2D6 (40  $\mu$ M). Hence, MRS5698 is generally stable in liver microsomes and has a low probability of causing significant drug–drug interactions. In both the Ames and hERG tests, MRS5698 was classified as “undefined” (Table 7), which means our calculations may not correctly predict its mutagenicity and cardiotoxicity. Tosh et al.<sup>43</sup> performed a non-GLP bacterial reversed mutation assay on MRS5698 and found it did not produce mutagenic effects on strains TA97, TA98, TA100, and TA102. Hence, the possibility of causing mutagenic effects in humans is low. The group also evaluated the inhibition activity of MRS5698 on the hERG channel and obtained an IC<sub>50</sub> value of 12  $\mu$ M. This suggests a low possibility of causing cardiac arrhythmias, which is one of the major safety factors leading to the withdrawal of prescription drugs worldwide<sup>50</sup>.

MRS5698 fulfills all the criteria for drug-like physicochemical properties except MW, which is slightly higher than the general cutoff weight of 500 (Table 6). This MW value is not necessarily a factor indicating poor bioavailability<sup>51</sup>, especially given that the Drug-Likeness and Molecular Property Prediction software indicated promising drug-like properties. The drug-likeness score for MRS5698 calculated by the software was 1.54, which suggests that MRS5698 has drug-like properties similar to most marketed medicines<sup>37</sup>.

Several in vitro and in vivo studies have demonstrated the analgesic therapeutic effects of MRS5698 on chronic pain, including metastatic cancer pain, chemotherapy-induced neuropathy, and nerve injury<sup>52</sup>. With regard to

cancer treatment, no published literature was found in searches of PubMed, the Cochrane Library, Google Scholar, and Science Direct. We therefore believe that this study is the first to suggest the anticancer effects, especially on endometrial cancer, of MRS5698.

Furthermore, MRS5698 can be synthesized on a large multigram scale at reasonable cost<sup>43</sup>. Given the pharmacological, pharmacodynamic, and pharmacokinetic parameters suggested by this study and the published literature, MRS5698 has high potential for further in vitro and in vivo investigation with the aim of developing safe and high-efficacy cancer treatment.

Another two compounds of note are 2-chloroadenosine and 2'-Me-CCPA (Fig. 6). Like MRS5698, they have higher binding affinities for A<sub>3</sub>AR and a lower affinity for ADA than cordycepin. Hence, they may exert anticancer effects with less ADA metabolism. The potential advantages of these compounds over MRS5698 are their lower MW (<500) (Table 6) and much lower PPB% and the fact that they are noninhibitors of all five CYP isoforms. However, both have higher ADA affinities than MRS5698, and 2-chloroadenosine has a low HIA value (Table 5). Nevertheless, the promising properties of 2-chloroadenosine and 2'-Me-CCPA indicate the worthiness of further investigations after the further investigation of MRS5698.

In conclusion, this study discovered the inhibitory effects of cordycepin on endometrial cancer cells. The effects were achieved by inducing the arrest of G<sub>0</sub>/G<sub>1</sub> phase cells and causing cellular apoptosis. Combinations of cordycepin and cisplatin possessed better antitumor effects in terms of inhibiting the proliferation of cancer cells, inducing cellular apoptosis, and regulating the cell cycle than the single compounds. This synergistic effect clearly exposes the potential of cordycepin as an adjunctive therapy with cisplatin, which may reduce the required chemotherapy dosage and hence reduce the adverse reactions caused by the drug.

The in silico simulations of binding affinities and drug-likeness properties on compounds with similar chemical structures to cordycepin revealed several potential drug candidates for cancer treatment. The most promising compound is MRS5698, followed by 2'-Me-CCPA and 2-chloroadenosine. Like cordycepin, they are able to stimulate the activities of A<sub>3</sub>AR, but with less metabolism by ADA. They also have acceptable drug-likeness and safety profiles. Further investigation and optimization of these compounds could contribute to the development of novel treatments for endometrial cancer.

*ACKNOWLEDGMENT: The financial support of the Macao Polytechnic Institute Research Fund (Project No. RP/ESS-04/2017) is gratefully acknowledged. The authors declare no conflicts of interest.*

## REFERENCES

1. Nevadunsky NS, Van Arsdale A, Strickler HD, Moadel A, Kaur G, Levitt J, Girda E, Goldfinger M, Goldberg GL, Einstein MH. Obesity and age at diagnosis of endometrial cancer. *Obstet Gynecol.* 2014;124:300–6.
2. Yin D, Jiang Y, Zhang S, Wang N, Lu Y, Wei H, Huo N, Xiao Q, Ou Y. No association between p21 gene rs1059234 polymorphisms and risk of endometrial cancer among Han women in Northeast China. *Cell Biochem Biophys.* 2015;71:167–71.
3. US National Cancer Institute. SEER Stat Fact Sheets: Endometrial cancer. Available from <http://seercancer.gov/statfacts/html/corphtml>.
4. Li X, Yang G, Li X, Zhang Y, Yang J, Chang J, Sun X, Zhou X, Guo Y, Xu Y. Traditional Chinese medicine in cancer care: A review of controlled clinical studies published in Chinese. *PLoS One* 2013;8:e60338.
5. Zhao X, Zheng X, Fan T, Li Z, Zhang Y, Zheng J. A novel drug discovery strategy inspired by traditional medicine philosophies. *Science* 2015;347:S38–40.
6. Elkady AI, Abu-Zinadah OA, Hussein RA. Crude flavonoid extract of medicinal herb *Zingibar officinale* inhibits proliferation and induces apoptosis in hepatocellular carcinoma cells. *Oncol Res.* 2017;25:897–912.
7. Tuli HS, Sharma AK, Sandhu SS, Kashyap D. Cordycepin: A bioactive metabolite with therapeutic potential. *Life Sci.* 2013;93:863–9.
8. Seong DB, Hong S, Muthusami S, Kim W, Yu J, Park W. Cordycepin increases radiosensitivity in cervical cancer cells by overriding or prolonging radiation-induced G2/M arrest. *Eur J Pharmacol.* 2016;771:77–83.
9. Nakamura K, Shinozuka K, Yoshikawa N. Anticancer and antimetastatic effects of cordycepin, an active component of *Cordyceps sinensis*. *J Pharmacol Sci.* 2015;127:53–6.
10. Fishman P, Bar-Yehuda S, Liang BT, Jacobson KA. Pharmacological and therapeutic effects of A3 adenosine receptor agonists. *Drug Discov Today* 2012;17:359–66.
11. Gessi S, Cattabriga E, Avitabile A, Gafa' R, Lanza G, Cavazzini L, Bianchi N, Gambari R, Feo C, Liboni A, Gullini S, Leung E, Mac-Lennan S, Borea PA. Elevated expression of A3 adenosine receptors in human colorectal cancer is reflected in peripheral blood cells. *Clin Cancer Res.* 2004;10:5895–901.
12. Morello S, Petrella A, Festa M, Popolo A, Monaco M, Vuttariello E, Chiappetta G, Parente L, Pinto A. Cl-IB-MECA inhibits human thyroid cancer cell proliferation independently of A3 adenosine receptor activation. *Cancer Biol Ther.* 2008;7:278–4.
13. Fishman P, Cohen S. The A3 adenosine receptor (A3AR): Therapeutic target and predictive biological marker in rheumatoid arthritis. *Clin Rheumatol.* 2016;35:2359–62.
14. Fishman P, Bar-Yehuda S, Farbstein T, Barer F, Ohana G. Adenosine acts as a chemoprotective agent by stimulating G-CSF production: A role for A1 and A3 adenosine receptors. *J Cell Physiol.* 2000;183:393–8.
15. Fishman P, Bar-Yehuda S, Vagman L. Adenosine and other low molecular weight factors released by muscle cells inhibit tumor cell growth. *Cancer Res.* 1998;58:3181–7.
16. Ciancetta A, Jacobson K. A structural probing and molecular modeling of the A3 adenosine receptor: A focus on agonist binding. *Molecules* 2017;22:449.
17. Keibel A, Singh V, Sharma MC. Inflammation micro-environment and the immune system in cancer progression. *Curr Pharm Des.* 2009;15:1949–55.
18. Tao X, Ning Y, Zhao X, Pan T. The effects of cordycepin on the cell proliferation migration and apoptosis in human lung cancer cell lines A549 and NCI-H460. *J Pharm Pharmacol.* 2016;68:901–11.
19. Li G, Nakagome I, Hirono S, Itoh T, Fujiwara R. Inhibition of adenosine deaminase (ADA)-mediated metabolism of cordycepin by natural substances. *Pharmacol Res Perspect.* 2015;3:e00121.
20. Saboury AA, Divsalar A, Jafari GA, Moosavi-Movahedi AA, Housaindokht MR, Hakimelahi GH. A product inhibition study on adenosine deaminase by spectroscopy and calorimetry. *J Biochem Mol Biol.* 2002;35:302–5.
21. Cui J, Culbertson R, Mao Z, Mock B. A novel therapeutic treatment utilizing cordycepin and cladribine synergy to decrease adverse treatment effects in various cancer cell lines. *J Exper Second Sci.* 2013;2:20–4.
22. Franken NA, Rodermond HM, Stap J, Haveman J, van Bree C. Clonogenic assay of cells in vitro. *Nat Protoc.* 2006;1:2315–9.
23. Chou TC. Drug combination studies and their synergy quantification using the Chou-Talalay method. *Cancer Res.* 2010;70:440–6.
24. Fong P, Tong HH, Chao CM. In silico prediction of tyrosinase and adenylyl cyclase inhibitors from natural compounds. *Nat Prod Commun.* 2014;9:189–94.
25. Southan C, Sharman JL, Benson HE, Faccenda E, Pawson AJ, Alexander SP, Buneman OP, Davenport AP, McGrath JC, Peters JA, Spedding M, Catterall WA, Fabbro D, Davies JA. The IUPHAR/BPS Guide to PHARMACOLOGY in 2016: Towards curated quantitative interactions between 1300 protein targets and 6000 ligands. *Nucleic Acids Res.* 2016;44:D1054–68.
26. Floris M, Sabbadin D, Medda R, Bulfone A, Moro S. Adenosiland: Walking through adenosine receptors landscape. *Eur J Med Chem.* 2012;58:248–57.
27. Deganutti G, Cuzzolin A, Ciancetta A, Moro S. Understanding allosteric interactions in G protein-coupled receptors using supervised molecular dynamics: A prototype study analysing the human A3 adenosine receptor positive allosteric modulator LUF6000. *Bioorg Med Chem.* 2015;23:4065–71.
28. Federico S, Redenti S, Sturlese M, Ciancetta A, Kachler S, Klotz KN, Cacciari B, Moro S, Spalluto G. The influence of the 1-(3-trifluoromethyl-benzyl)-1H-pyrazole-4-yl moiety on the adenosine receptors affinity profile of pyrazolo[4,3-e][1,2,4]triazolo[1,5-c]pyrimidine derivatives. *PLoS One* 2015;10:e0143504.
29. Jones G, Willett P, Glen RC, Leach AR, Taylor R. Development and validation of a genetic algorithm for flexible docking. *J Mol Biol.* 1997;267:727–48.
30. Korb O, Stutzle T, Exner TE. Empirical scoring functions for advanced protein-ligand docking with PLANTS. *J Chem Inf Model* 2009;49:84–96.
31. Li Y, Han L, Liu Z, Wang R. Comparative assessment of scoring functions on an updated benchmark: 2. Evaluation methods and general results. *J Chem Inf Model* 2014;54:1717–36.
32. Chen YC. Beware of docking! *Trends Pharmacol Sci.* 2015;36:78–95.

33. Irwin JJ, Sterling T, Mysinger MM, Bolstad ES, Coleman RG. ZINC: A free tool to discover chemistry for biology. *J Chem Inf Model* 2012;52:1757–68.
34. Fong P, Tong HH, Ng KH, Lao CK, Chong CI, Chao CM. In silico prediction of prostaglandin D2 synthase inhibitors from herbal constituents for the treatment of hair loss. *J Ethnopharmacol*. 2015;175:470–80.
35. Kuok CF, Hoi SO, Hoi CF, Chan CH, Fong IH, Ngok CK, Meng LR, Fong P. Synergistic antibacterial effects of herbal extracts and antibiotics on methicillin-resistant *Staphylococcus aureus*: A computational and experimental study. *Exp Biol Med*. (Maywood) 2017;242:731–43.
36. ACD/Percepta version 140, 2015. Available from <https://www.acdlabs.com/>
37. Molsoft LLC. Drug-likeness and molecular property prediction [cited 2017 Jun 6]. Available from <http://molsoft.com/mprop>
38. Xu C, Cheng F, Chen L, Du Z, Li W, Liu G, Lee P W, Tang Y. In silico prediction of chemical Ames mutagenicity. *J Chem Inf Model* 2012;52:2840–7.
39. Jing Y, Easter A, Peters D, Kim N, Enyedy IJ. In silico prediction of hERG inhibition. *Future Med Chem*. 2015; 7:571–86.
40. Hagenow S, Stasiak A, Ramsay R, Stark H. Ciproxifan a histamine H3 receptor antagonist reversibly inhibits monoamine oxidase A and B. *Sci Rep*. 2017;7:40541.
41. El-Miligy MM, Hazzaa AA, El-Messmary H, Nassra RA, El-Hawash SA. New benzothioephene derivatives as dual COX-1/2 and 5-LOX inhibitors: Synthesis biological evaluation and docking study. *Future Med Chem*. 2017;9: 443–68.
42. Li J, Jiang K, Qiu X, Li M, Hao Q, Wei L, Zhang W, Chen B, Xin X. Overexpression of CXCR4 is significantly associated with cisplatin-based chemotherapy resistance and can be a prognostic factor in epithelial ovarian cancer. *BMB Rep*. 2014;47:33–8.
43. Tosh DK, Padia J, Salvemini D, Jacobson KA. Efficient large-scale synthesis and preclinical studies of MRS5698, a highly selective A3 adenosine receptor agonist that protects against chronic neuropathic pain. *Purinergic Signal*. 2015;11:371–87.
44. Tosh DK, Deflorian F, Phan K, Gao Z G, Wan TC, Gizewski E, Auchampach JA, Jacobson KA. Structure-guided design of A(3) adenosine receptor-selective nucleosides: Combination of 2-arylethynyl and bicyclo[3.1.0]hexane substitutions. *J Med Chem*. 2012;55:4847–60.
45. Paoletta S, Tosh DK, Salvemini D, Jacobson KA. Structural probing of off-target G protein-coupled receptor activities within a series of adenosine/adenine congeners. *PLoS One* 2014;9:e97858.
46. Little JW, Ford A, Symons-Liguori AM, Chen Z, Janes K, Doyle T, Xie J, Luongo L, Tosh DK, Maione S, Bannister K, Dickenson AH, Vanderah TW, Porreca F, Jacobson KA, Salvemini D. Endogenous adenosine A3 receptor activation selectively alleviates persistent pain states. *Brain* 2015;138:28–35.
47. Jin ML, Park SY, Kim YH, Oh JI, Lee SJ, Park G. The neuroprotective effects of cordycepin inhibit glutamate-induced oxidative and ER stress-associated apoptosis in hippocampal HT22 cells. *Neurotoxicology* 2014;41:102–11.
48. Scheife RT. Protein binding: What does it mean? *DICP* 1989;23:S27–31.
49. Roder BL, Frimodt-Moller N, Espersen F, Rasmussen SN. Dicloxacillin and flucloxacillin: Pharmacokinetics protein binding and serum bactericidal titers in healthy subjects after oral administration. *Infection* 1995;23:107–12.
50. Fung M, Thornton A, Mybeck K, Wu JH, Hornbuckle K, Muniz E. Evaluation of the characteristics of safety withdrawal of prescription drugs from worldwide pharmaceutical markets—1960 to 1999. *Drug Inf J*. 2001;35:293–317.
51. Veber DF, Johnson SR, Cheng HY, Smith BR, Ward KW, Kopple KD. Molecular properties that influence the oral bioavailability of drug candidates. *J Med Chem*. 2002;45:2615–23.
52. Salvemini D, Janes K, Finley A, Doyle T, Chen Z, Bryant L, Tosh D, Jacobson K. Adenosine receptor subtype 3 (A3AR) agonists as novel analgesics in chronic neuropathic pain. *FASEB J*. 2013;27:887.1.